catalysts

MDPI

Article

Catalytic Cracking of Fischer-Tropsch Wax on Different Zeolite Catalysts

Chao Yang, Lingtao Liu *, Genquan Zhu, Chaogang Xie, Xiance Zhang and Xiaoqiao Zhang

Sinopec Research Institute of Petroleum Processing Co., Ltd., Beijing 100083, China
* Correspondence: liult.ripp@sinopec.com; Tel.: +86-010-82369225

Abstract: Fisher-Tropsch synthesis (FTS) is a promising method to make alternative hydrocarbons from biomass or other resources. Upgrading the primary FTS products is of considerable interest. Cracking FT wax is economically attractive to produce light olefins. Herein, the effects of the zeolite type, Si/Al ratio of ZSM-5, and reaction condition on the catalytic cracking of FT wax were investigated. It was found that the pore structure and acid properties of zeolites had a significant impact on the product selectivity. USY was beneficial for the production of gasoline and diesel, while β was suitable for the production of propylene and butenes, and ZSM-5 was conductive to producing ethylene and propylene. Increasing the Si/Al ratio of ZSM-5 can suppress the hydrogen transfer reaction and increase the selectivity of light olefins. When the Si/Al ratio of ZSM-5 was 140, the mass yields of ethylene, propylene, and butenes were 6.40%, 26.83%, and 20.10%, respectively.

Keywords: Fisher-Tropsch wax; catalytic cracking; light olefins; zeolite; Si/Al ratio

1. Introduction

Ethylene and propylene are the building blocks of the petrochemical industry as they can be turned into plastics, fiber, lubricates, and so on. At present, the dominant processes for producing these light olefins are steam cracking and fluid catalytic cracking. Propane dehydrogenation (PDH) [1–4] and methanol-to-olefin (MTO) [5–9] have also emerged as new routes to producing propylene and/or ethylene. As the consumption of gasoline and diesel is decreasing in many countries and areas, producing light olefins from heavy oil using the fluid catalytic cracking unit (FCCU) is attractive for many companies [10]. Deep catalytic cracking (DCC), developed by the Research Institute of Petroleum Processing (RIPP) of SINOPEC, is regarded as a bridge between refinery and chemicals [11–14]. Other technology based on the FCCU, such as Maxofin FCC, PetroFCC, and HS-FCC are also utilized to produce light olefins.

It has been widely recognized that the molecular structures of feedstock are one of the crucial factors used to determine light olefins yield in catalytic cracking. Paraffins with a high molecular weight are ideal feedstock for producing light olefins, while the aromatics normally give a lower light olefins yield.

Zeolites, which contain internal porous structures with acid sites, are the main active component of the FCC catalyst or additives. During the reaction, large molecules are cracked to the desired fractions using different types of zeolites. Zeolite Y, with a 7 Å diameter pore and 12 Å diameter cavity, are commonly used for producing gasoline [15]. For the production of light olefins, ZSM-5 is the most widely used active phase or additive [16]. Beta is usually used for increasing the yield of C4 fractions in the FCCU [17,18].

Fisher-Tropsch synthesis (FTS) is an alternative method for producing hydrocarbons from syngas derived from coals, biomass, waste plastics, etc. [19,20]. It has been commercialized in many places, such as South Africa and China. FTS products have quite different molecular structures from petroleum. The product distribution of traditional FTS normally follows the Anderson-Schulz-Flory distribution and is mainly paraffin, olefin, and a small

check for updates

Citation: Yang, C.; Liu, L.; Zhu, G.; Xie, C.; Zhang, X.; Zhang, X. Catalytic Cracking of Fischer-Tropsch Wax on Different Zeolite Catalysts. *Catalysts* **2023**, *13*, 1223. https://doi.org/10.3390/catal13081223

Academic Editor: Izabela Czekaj

Received: 27 July 2023
Revised: 11 August 2023
Accepted: 16 August 2023
Published: 18 August 2023

amount of oxygenates [20–22]. The low-temperature FTS process would produce almost 50 wt% of FT wax [23]. Along with the vigorous development of FTS in the industrial field, modified-FTS for the conversion of captured CO_2 and green H_2 to produce carbon-neutral liquid fuels is widely investigated as it avoids using syngas from fossil fuels and reduces CO_2 emissions [24–27]. During these processes, FT wax is also regarded as an undesired product. It cannot be directly used as transportation fuel as it is a mixture of long chain hydrocarbons and has significant differences in its physical properties. Hydrocracking is a commonly used approach. FT wax can be hydrocracked to aviation kerosene, diesel oil, etc. High-quantity lube base oil is also produced using hydro-isomerization dewaxing technology [28–31]. However, the hydrocracking process requires high operation pressure and high hydrogen consumption, which reduces its economy. It can also be directly used to produce special wax with high added value, but its market capacity is very limited. Thus, improving the value of FT wax is an important topic for the vigorous development of FTS technology.

Catalytic cracking FT wax to light olefins in the FCCU is an attractive option. Xander Dupain et al. used the combination of an equilibrium catalyst with a steam-deactivated ZSM-5 additive to evaluate cracking FT wax in the FCCU and found that the gasoline yield could reach as high as 70 wt%. In an optimized condition, 16 wt% propylene and 15 wt% butenes were achieved [32,33]. V. G. Komvokis et al. reported the cracking of FT wax on different zeolitic and mesoporous aluminosilicate catalytic materials, and found that the micropore structure/size of the zeolites had a significant effect on the conversion and product yields [34]. M. Yang et al. studied FT wax catalytic cracking in a pilot-scale riser and turbulent fluidized bed [35]. The yields of gasoline and liquefied petroleum gases (LPG, total C3 and C4) reached 50.40 wt% and 42.94 wt%, respectively. W. Zhao et al. used an industrial β-zeolite-based catalyst to crack FT wax in a riser reactor, and the LPG yield was nearly 40 wt% [36].

Light olefins, especially ethylene and propylene, are still in demand in many areas. In this study, the effect of the zeolites and reaction parameters were studied to achieve a higher yield of ethylene and propylene.

2. Results

2.1. Catalyst Properties

From Table 1, it can be found that the surface areas of the catalysts were in the range of 304~404 m^2/g, and the pore volumes were 0.167~0.266 cm^3/g. As shown in Figure 1, the N_2 adsorption-desorption isotherms of Cat-Z5-X and Cat-β exhibited type I physisorption, corresponding to a typical microporous structure, while that of Cat-USY was type IV, corresponding to a mesoporous structure.

Table 1. Properties of catalysts.

Catalysts	Cat-USY	Cat-β	Cat-Z5-40	Cat-Z5-90	Cat-Z5-140
Surface area/(m^2/g)	371	304	336	397	404
Pore volume/(cm^3/g)	0.177	0.266	0.167	0.193	0.204
Compositions/wt%					
Al_2O_3	22.70	7.46	6.95	3.38	2.26
SiO_2	74.6	92.3	85.8	88.4	93.2
Na_2O	0.87	0.01	0.03	0.08	0.05

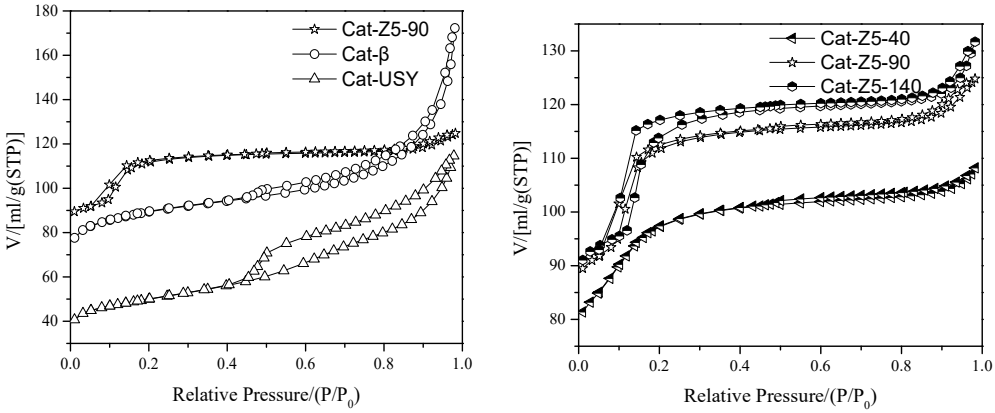

Figure 1. Nitrogen adsorption-desorption isotherms and porosity characteristics of catalysts.

Table 2 presents the FT-IR acidity analysis results. It can be noticed that the acid content of Cat-USY was much higher than the other catalysts. However, its strong acid ratio was the lowest. In the case of the ZSM-5 catalyst, with the increase in Si/Al, the total acid content decreased, while the strong acid ratio increased.

Table 2. Acidity properties of ZSM-5 with different Si/Al ratio.

Unit: μmol/g	Weak Acid		Strong Acid		Total	Strong Acid/ Weak Acid
	Brønsted	Lewis	Brønsted	Lewis		
Cat-USY	11.2	13.8	6.6	14.3	45.9	0.84
Cat-β	1.5	4.9	2.4	3.9	12.7	0.98
Cat-Z5-40	12.5	1.3	9.4	5.3	28.5	1.07
Cat-Z5-90	4.6	1.2	4.2	3.1	13.1	1.26
Cat-Z5-140	0.2	0.2	0.7	0.8	1.9	3.75

2.2. Cracking FT Wax on Different Zeolite Catalysts

Table 3 presents the conversion and product distribution of cracking FT wax using catalysts with different zeolites. It can be seen that up to 90% of the conversions were obtained over all the studied catalysts. FT wax, which is mainly comprised of normal alkanes, has an average molecular dynamics diameter of between 0.43 nm~0.50 nm [37]. The pore structure size of the zeolite of the catalysts was USY > β > ZSM-5, wherein the pore diameter of the ZSM-5 zeolite was 0.54 nm × 0.56 nm; thus, the FT wax could easily enter the pore channel of all three zeolites and could be cracked by the acid sites.

Table 3. Product distribution on different catalysts.

	Cat-USY	Cat-β	Cat-Z5-90
Yield/%			
Dry gas	1.45	2.98	7.28
LPG	45.90	54.96	56.55
Gasoline	43.40	40.98	33.06
Diesel	7.97	0.82	1.82
Heavy oil	0.65	0.00	1.15
Coke	0.63	0.25	0.14
Conversion/%	91.38	99.18	97.03
Light olefins yield/%			
Ethylene	1.05	2.30	6.92
Propylene	18.05	23.27	25.91
Butenes	20.39	24.22	19.17
Total light olefins	39.50	49.78	52.01
$(C_3^= + C_4^=)/(C_3 + C_4)$	0.84	0.86	0.80

However, the product distribution varied dramatically. With Cat-USY, the yields of gasoline and diesel were 43.40 wt% and 7.97 wt%, respectively, which were much higher than those with Cat-β and Cat-Z5-90. The conversion of FT wax to light olefins on Cat-β was similar to that of Cat-Z5-90, and higher than that on Cat-USY. Compared to Cat-Z5-90, the dry gas yield on Cat-β was reduced by 4.30% and the butenes yield increased by 5.05%. With Cat-Z5-90, the yields of dry gas and LPG were 7.28 wt% and 56.55 wt%, of which the ethylene yield was 6.92 wt% and the propylene yield was 25.91 wt%.

The difference of the product distribution was due to the physicochemical properties of the zeolite. The USY zeolite is composed of a series of spherical cavities with a diameter of about 1.2 nm, which is conducive to the diffusion of large wax molecules and reaction intermediates, thus improving the selectivity of the gasoline and diesel yields in the products. The β zeolite is composed of two types of channels, one with a pore diameter of about 0.73 nm × 0.60 nm in the horizontal direction and the other with a twisted channel with a diameter of about 0.56 nm × 0.56 nm in the vertical direction. The relatively large twelve-membered ring straight channels in the β zeolite are sterically favorable for the isomerization of hydrocarbon molecules, thereby promote the formation of butenes. ZSM-5 is a mesoporous zeolite, characterized by a 10-membered ring pore structure which greatly strengthens the cracking and isomerization reaction of hydrocarbon molecules. It has been widely used as a promoter for increasing propylene and high-octane additives. From Table 2, it can be seen that Cat-Z5-90 had a much higher ratio of Brønsted acid sites to Lewis acid sites than both Cat-USY and Cat-β, which would also influence the cracking reaction. The high strong/weak acid ratio was beneficial for increasing the light olefins yield as the order of the ratio was Cat-Z5-90 > Cat-β > Cat-USY, showing a similar tend to the change in the light olefins yield. Thus, it can be concluded that the different pore structures and the acid characters were the crucial factors to determine the product distribution of FT wax cracking. In addition, the size and morphologies of the zeolites' crystals can also affect the product distribution during catalytic cracking [38,39]. Y. Hirota et al. reported that 75 nm-sized SAPO-34 nanocrystals showed a longer catalyst lifetime in both MTO and dimethylether-to-olefins (DTO) reactions than the 800 nm-sized SAPO-34 [40]. A multi-edge morphology and hierarchical porous structure are also found to be advantageous for the DTO reaction [41]. The possible reason for the superior performance of the zeolite was a short residence time for products because of a shorter diffusion length. This might also influence the product distribution in FT wax cracking.

In addition to the differences in the fractions, the detailed composition also changed with the zeolite types. The compositions of the dry gas and LPG are shown in Table 4. On Cat-Z5-90, 95.14 wt% of the dry gas was ethylene, 55.54 wt% of the LPG was C_3, of which 45.83 wt% was propylene; these rates were significantly higher than those on Cat-USY and Cat-β. The yield of propylene using Cat-β was slightly lower than that of Cat-Z5-90, but the mass fraction of butenes in its LPG was as high as 44.01 wt%, of which the isobutene fraction was 18.60 wt%. The yield and selectivity of butenes on Cat-β were significantly higher than those on Cat-Z5-90. Among the three catalysts, Cat-Z5-90 was suitable for producing ethylene and propylene, while Cat-β was suitable for propylene and butenes.

Table 5 lists the gasoline composition on different types of zeolite catalysts. With the decrease in the pore size of the zeolites, the mass fractions of *n*-paraffins, olefins, naphthenes, and aromatics in the gasoline all increased, while the mass fraction of *i*-paraffins decreased. The content of both weak and strong acid was higher on Cat-USY than Cat-β and Cat-Z5-90; additionally, its large cavity was conducive to the hydrogen transfer reaction. Although the total acid content of Cat-Z5-90 was less than Cat-USY, the fraction of strong acid was the highest, which was conducive to cracking, while the hydrogen transfer activity was relatively low. Compared with Cat-Z5-90, the fraction of strong acid over Cat-β was lower, resulting in a mild cracking performance of gasoline. The hydrogen transfer index of Cat-USY, Cat-β, and Cat-Z5-90 were 0.58, 0.37, and 0.35, respectively.

Table 4. Composition of dry gas and LPG on different catalysts.

	Cat-USY	Cat-β	Cat-Z5-90
Dry gas/wt%			
Hydrogen	1.58	5.93	0.64
Methane	13.62	11.82	1.34
Ethane	12.31	5.21	2.88
Ethylene	72.49	77.04	95.14
LPG/wt%			
Propane	3.09	3.31	9.71
Propylene	39.31	42.34	45.83
i-Butane	10.20	7.14	4.90
n-Butane	2.97	3.14	5.66
n-Butene	8.56	8.17	6.20
i-Butene	16.96	18.60	13.59
trans-2-Butene	10.86	9.92	8.05
cis-2-Butene	8.04	7.32	5.82
1,3-Butadiene	0.01	0.05	0.24

Table 5. Group compositions of gasoline on different catalysts.

	Cat-USY	Cat-β	Cat-Z5-90
Group compositions/%			
n-alkanes	13.67	14.78	17.56
i-alkanes	27.53	15.36	7.47
olefins	35.59	42.32	43.72
naphthenes	2.12	2.37	5.09
aromatics	21.09	25.17	26.16
C_{HT}	0.58	0.37	0.35

The mass fraction of aromatics in gasoline obtained by the three different types of zeolite catalysts were all less than 30%; this is much lower than the traditional DCC process's gasoline, which is usually up to 50%. C. J. Mota summarized the previous understanding of gasoline aromatics and studied the reaction mechanism through experiments [42]. It was found that in the initial stage of cracking, the aromatics in gasoline mainly came from the dealkylation reaction of monocyclic aromatics in the reactant. When the conversion increased, the olefins in the gasoline increased, and secondary reactions such as hydrogen transfer and cyclodehydrogenation increased to generate gasoline aromatics. FT wax does not contain cyclic compounds, such as aromatic and naphthenic hydrocarbons; thus, aromatics in gasoline should derive from the cyclodehydrogenation of olefins. Figure 2 shows the yields of aromatic hydrocarbons with different carbon numbers in gasoline. It can be seen that compared with Cat-USY and Cat-β, the yield of C6~C8 aromatics using Cat-Z5-90 was substantially improved, and the C9~C11 aromatics were remarkably reduced. The larger pore size of USY and β was beneficial for the formation of heavy aromatics, and Cat-Z5-90 was beneficial for producing light aromatics-BTX.

From the screening of the zeolite types above, among the three catalysts, Cat-Z5-90 had the highest yield of light olefins and light aromatics.

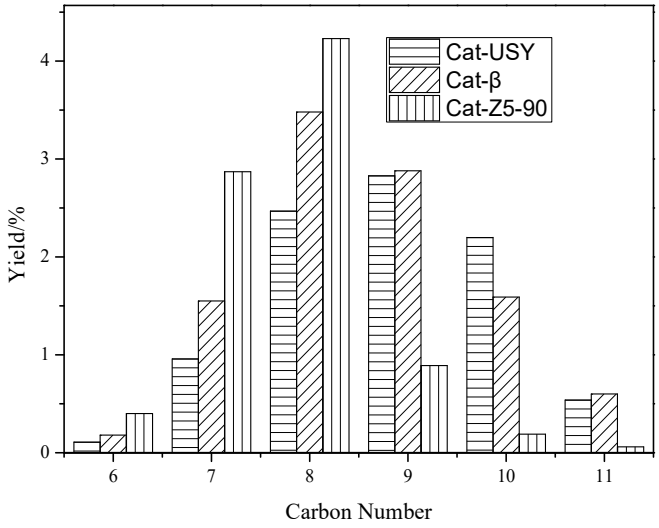

Figure 2. Yield of aromatics in gasoline on different catalysts.

2.3. Effect of Si/Al Ratio on Cracking

To further improve the yield of light olefins, cracking the olefins and paraffins in gasoline and suppressing the hydrogen transfer reaction would be the two feasible ways. As ZSM-5 had shown the highest light olefins yield in the above tests, we continued to study the effect of the Si/Al ratio of ZSM-5 on FT wax cracking.

The cracking performance of FT wax on ZSM-5 catalysts with different Si/Al ratios was investigated at 560 °C. The product distribution is given in Table 6. It can be seen that as the Si/Al ratio of ZSM-5 increased, the yield of diesel and heavy oil in the product increased, while the conversion decreased. This was attributed to the fact that with a higher Si/Al ratio, the acid content of ZSM-5 declined, leading to a lower conversion. The dry gas yield in the product significantly decreased, especially for the ethylene yield. It is generally believed that some parts of ethylene are produced by high-temperature thermal reactions from a free radical mechanism [43,44] and some are catalyzed by acids [45]. As the Si/Al ratio increased, the yield of LPG slightly increased, but the yield of propylene and butenes in the product notably increased. Using Cat-Z5-140, the yield of propylene was as high as 26.83%, and that of butenes reached 20.10%. The hydrogen transfer index was also reduced. Low acid density is conducive to inhibiting the hydrogen transfer reaction. On the whole, a high Si/Al ratio was favorable for increasing the yield and selectivity of light olefins. It can also be seen that the coke yield decreased with the Si/Al ratio. This was because a low acid density was conducive to inhibiting the hydrogen transfer reaction, which was the crucial reaction for coke formation. Nevertheless, the coke yields on the three catalysts were only ~0.1%, which is much lower than the traditional FCC process. As the coke deposit was one of the major factors for catalyst deactivation, it was reasonable to deduce that the deactivation would be minor.

In addition to the yield of individual fractions, their compositions were also important as they determined the downstream upgrading of the primary products. The detailed compositions of dry gas and LPG are given in Table 7. The ethylene concentration was above 90% in all cases, which is much higher than using VGO/HVGO derived from petroleum as feedstocks [10]. The mass fraction of paraffin in LPG decreased with the increasing Si/Al ratio, while the olefins, namely propylene and butenes, increased significantly. However, the mass fraction of the total C_3 and total C_4 hydrocarbons in the LPG remained almost unchanged.

Table 6. Product distribution on ZSM-5 with different Si/Al ratio.

	Cat-Z5-40	Cat-Z5-90	Cat-Z5-140
Yield/%			
Dry gas	10.78	7.28	6.75
LPG	56.04	56.55	57.24
Gasoline	31.01	33.06	32.75
Diesel	1.33	1.82	2.11
Heavy oil	0.68	1.15	1.05
Coke	0.16	0.14	0.10
Conversion/%	97.99	97.03	96.84
Light olefins yield/%			
Ethylene	10.03	6.92	6.40
Propylene	22.19	25.91	26.83
Butenes	15.00	19.17	20.10
Total light olefins	47.22	52.00	53.33
$(C_3^= + C_4^=)/(C_3 + C_4)$	0.66	0.80	0.82
C_{HT}/%	0.83	0.35	0.29

Table 7. Composition of dry gas and LPG on ZSM-5 with different Si/Al ratio.

	Cat-Z5-40	Cat-Z5-90	Cat-Z5-140
Dry gas/wt%			
Hydrogen	0.72	0.64	0.64
Methane	1.94	1.34	1.42
Ethane	4.29	2.88	3.16
Ethylene	93.05	95.14	94.78
LPG/wt%			
Propane	16.07	9.71	8.73
Propylene	39.58	45.83	46.89
i-Butane	8.88	4.90	4.20
n-Butane	8.69	5.66	5.07
n-Butene	4.92	6.20	6.43
i-Butene	10.28	13.59	14.14
trans-2-Butene	6.39	8.05	8.34
cis-2-Butene	4.72	5.82	6.01
1,3-Butadiene	0.47	0.24	0.19
C_3/LPG	0.56	0.56	0.56

Table 8 presents the group composition of gasoline. The mass fraction of alkanes and olefins in the gasoline increased with the increase in the Si/Al ratio, while the mass fraction of aromatics decreased. This indicated that the cyclization and dehydrogenation of olefins to aromatics were suppressed when the zeolite had a low acid density. This was consistent with the changes in the composition of the LPG.

Table 8. Group compositions of gasoline on ZSM-5 with different Si/Al ratio.

	Cat-Z5-40	Cat-Z5-90	Cat-Z5-140
Group compositions/%			
n-Alkanes	8.67	17.56	18.92
i-Alkanes	6.04	7.47	7.15
Olefins	40.43	43.72	50.97
Naphthenes	5.32	5.09	4.43
Aromatics	39.54	26.16	18.53

2.4. Effect of Space Velocity

During the catalytic cracking, the feedstock and intermediates underwent complex parallel and sequential reactions. The residence time, along with the temperature and

other factors, determined the degree of cracking severity. A too-high space velocity might result in insufficient time for feedstock cracking and further conversion of the intermediates, which has a negative effect on increasing light olefins. On the other hand, hydrogen transfer, aromatization, and other undesired reactions would be unremarkable. A low space velocity led to a more sufficient time for the feeding molecules to make contact with the catalyst, facilitating further conversion to light olefins, but also intensified the undesired reactions.

The catalytic cracking performance of FT wax under different weight hourly space velocities (WHSV) at 560 °C was investigated. The product distribution is shown in Table 9. The decrease in the WHSV resulted in the increased conversion of FT wax. When the WHSV decreased from 41 h^{-1} to 4 h^{-1}, the yield of dry gas and LPG both increased dramatically, much higher than the increasing ratio of the conversion. However, the yields of gasoline and diesel decreased. The opposite trend of changes illustrated that a large portion of dry gas and LPG were derived from gasoline and diesel. The coke yield remained almost unchanged, at around 1%.

Table 9. Product distribution at different WHSV.

WHSV/h^{-1}	**41**	**27**	**15**	**7**	**4**
Products/%					
Dry gas	1.27	1.39	2.02	2.95	4.35
Ethylene	0.91	1.06	1.55	2.30	3.35
LPG	33.84	43.03	49.86	54.05	57.45
Propane	1.41	1.95	2.24	2.52	2.78
Propylene	12.51	16.35	19.57	22.65	25.56
Butanes	4.28	5.64	6.81	7.25	7.16
Butenes	15.64	19.09	21.24	21.63	21.95
Gasoline	45.11	43.60	40.96	37.33	33.75
n-Alkanes	5.51	6.54	6.20	6.76	6.46
i-Alkanes	8.87	9.04	9.11	7.62	5.93
Olefins	25.74	20.28	15.91	9.44	6.90
Naphthenes	0.80	0.94	0.96	1.13	1.08
Aromatics	4.19	6.80	8.78	12.38	13.38
Diesel	15.17	10.46	6.25	4.56	3.35
Heavy oil	3.69	0.90	0.00	0.00	0.00
Coke	0.92	0.62	0.91	1.11	1.10
Conversion/%	81.14	88.64	93.75	95.44	96.65
Ethylene/Dry gas	0.83	0.76	0.77	0.78	0.77
C_{HT}	0.46	0.49	0.56	0.62	0.61

As the WHSV decreased, the yields of ethylene, propylene, and butenes all increased, but their rates of increase were different. The yield of butenes increased sharply between WHSVs of 41 h^{-1} and 15 h^{-1}, and the growth became sluggish between 15 h^{-1} and 4 h^{-1}. At high WHSVs, the yield of butenes was higher than that of propylene. As the reaction time prolonged, the yield of propylene significantly increased, and the yield of propylene was higher than that of butenes. The yields of propylene and butenes were influenced by both generation and consumption. In the initial stage, as the reaction time prolonged, the concentrations of propylene and butenes were quite low; thus, the consumption rate was minor, and the generation rates of propylene and butenes dominated their yields. As the reaction time continued to extend, the concentration of reactants to produce propylene and butenes decreased, resulting in a decrease in the generation rate. At the same time, as the concentration of propylene and butenes increased, the rate of consumption increased.

The WHSV also impacted the composition of gasoline. As the WHSV decreased, the hydrogen transfer index increased, the yield of olefins decreased, and that of aromatics increased. The FT wax mainly underwent the cracking reaction in the early stage of the reaction, and as the reaction time prolonged, the cracking reaction of large molecules intensified, accompanied by an enhanced hydrogen transfer reaction. When the reaction time continued to extend, the cracking reaction of the middle fraction intensified, the yield

of light olefins increased, while the hydrogen transfer reaction was strengthened, leading to high aromatic percentages.

3. Discussion

Figure 3 presents a schematic diagram of the pathway for the catalytic cracking of FT wax to produce light olefins. There were two main pathways for light olefins production: one was the cracking of FT wax in a single step to generate light olefins (pathway 1). The other was the cracking of intermediate products, such as diesel or gasoline, to produce light olefins (pathway 2). The catalytic cracking of FT wax followed both the single molecular and bimolecular cracking mechanisms, which involved the carbonium ion and carbenium ion [16]. The single molecular mechanism proceeds when the proton on the catalyst attacks the C-C or C-H bond of an alkane to form a pentacoordinated carbonium ion, and then decomposes to H_2 or a small alkane and a carbenium ion. Bimolecular cracking takes place when a carbenium reacts with the FT wax or intermediate products through the H-transfer step to form an alkane and a small carbenium ion. The carbenium ion can further form an olefin and a smaller carbenium ion through β-scission or form olefin with the same carbon number. Thermal cracking takes place through the free radical mechanism at elevated temperatures. The zeolite properties, including the structure (e.g., pore structures, cavities) and chemical properties (Si/Al ratio, acidity distribution, etc.), together with the reaction conditions, influence the product distribution.

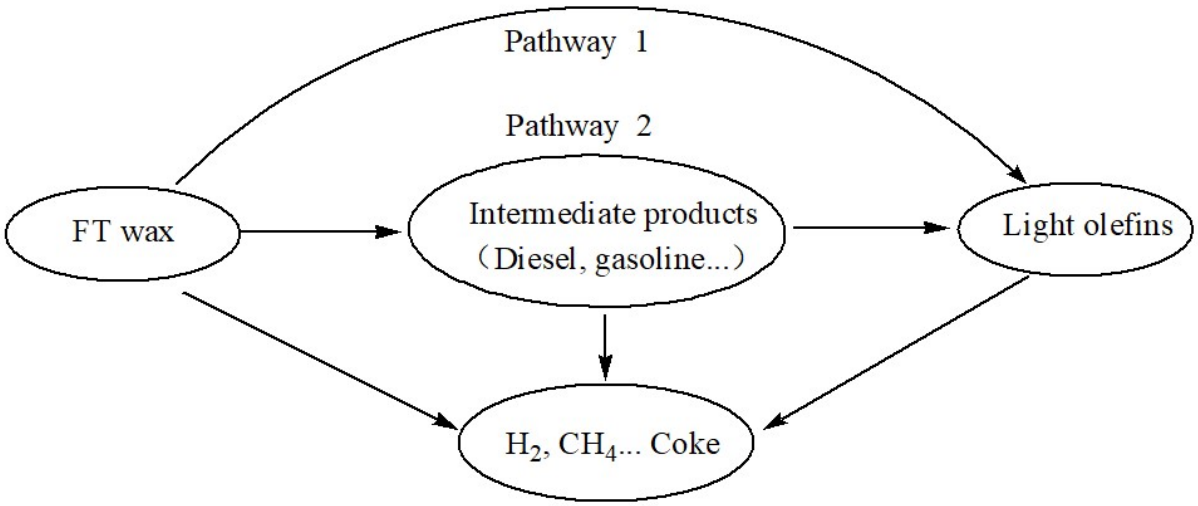

Figure 3. Pathway of light olefins producing from FT wax.

Based on the changes in the light olefins yield, it can be concluded that in the low conversion stage of FT wax cracking, light olefins were mainly obtained through pathway 1. As the conversion increased, a large number of middle distillates were generated, and the proportion of secondary cracking in the generation of light olefins increased (pathway 2). The cracking of olefins in gasoline played a major role in the second pathway.

4. Materials and Methods

4.1. Materials

The raw material used in this work is the heavy part of the low-temperature FTS, namely FT wax. It was purchased from Shaanxi Future Energy and Chemicals Co., Ltd., Yulin City, China. Table 10 lists its main properties. The hydrogen mass fraction of the FT wax was 14.47%, much higher than the petroleum-based FCC feedstocks, and 80.6% of the hydrocarbon composition is *n*-alkanes. It had a broad range carbon number distribution (Figure 4), the distribution of which concentrated between 20~50.

Table 10. Properties of the feed oil.

ρ^{20}/(kg·m^{-3})	*w*(Element)/%			Distillation Data of ASTM D-2887/°C					*w*(*n*-Alkanes)/%
	C	H	O	IBP	10%	30%	50%	90%	
806	85.18	14.47	0.35	268	391	465	521	652	80.6

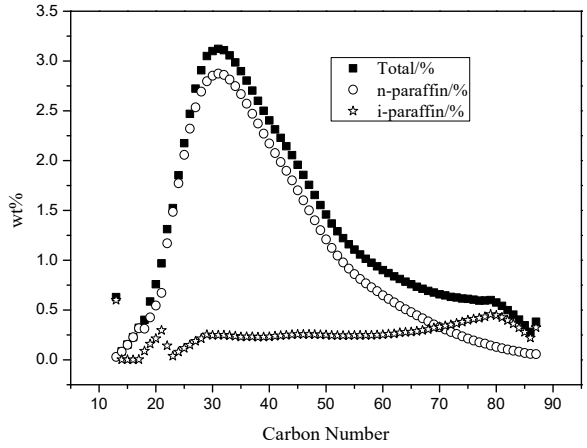

Figure 4. Carbon number distribution of FT wax.

4.2. Catalyst

Catalysts with USY, β, and ZSM-5 zeolites as active phases (50% mass fraction) were labeled as Cat-USY and Cat-β, and Cat-Z5-X, respectively, where X refers to the Si/Al ratio (molar). All zeolites were purchased from Sinopec Research Institute of Petroleum Processing Co., Ltd (Beijing, China). Before testing and analyzing, all catalysts were hydrothermally aged at 800 °C for 8 h with 100% steam.

N_2 adsorption–desorption experiments were conducted on Micromeritics, ASAP 2420. The Brunauer-Emmett-Teller (BET) equation was used to calculate the surface areas of the samples.

Fourier transform infrared (FT-IR) spectroscopy experiments (Bruker, VERTEX 70) were conducted to examine the Brønsted and Lewis acid sites of the samples. After pyridine desorption at 200 °C and 350 °C, the concentration of the total and strong Lewis/Brønsted acid site is obtained from the integrated absorbance of the respective bands. The concentration of Brønsted acid and Lewis acid is determined by the infra-red absorption band of pyridine at 1540 cm^{-1} and 1453 cm^{-1}, respectively. The molar extinction coefficients were based on the work of C. A. Emers et al. [46].

4.3. Reaction Equipment

A multi-channel micro fixed bed reactor (MCC) was used for the evaluation, which was designed by the Institute of Petrochemical Science and manufactured by Shanghai Meryer Experimental Equipment Co., Ltd. It consisted of six parallel quartz tube reactors (Figure 5). Each reactor with a diameter of 6 mm was selected, and a 1.2 g catalyst was loaded for each test. The feeding oil entered the reactor through an injection pump, and the products were purged by N_2 to the liquid collection bottle for cooling and gas-liquid separation. After all reactors had completed the reaction, air was introduced into each reactor for regeneration. The coke deposited on the catalyst was burned and the flue gas entered the CO conversion furnace to be fully converted to CO_2. Then, the CO_2 content in the flue gas was measured using an online CO_2 infrared analyzer, and the coke yield was calculated based on the concentration of CO_2 and volume of flue gas.

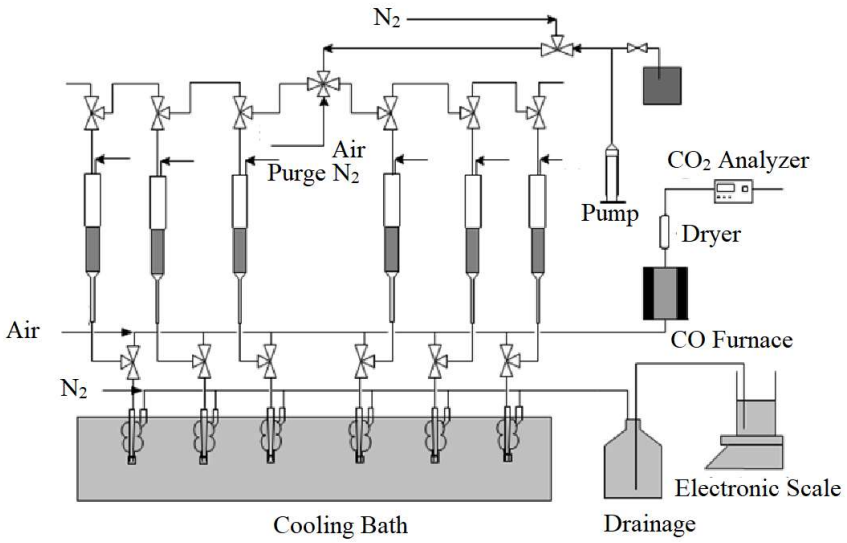

Figure 5. Multi-channel micro fixed bed reactor (MCC) flow diagram.

The cracking performance of FT wax on the three catalysts was investigated at 560 °C and 110 kPa (absolute).

4.4. Analysis

The volumetric percentage of each component in the vapor was determined using an Agilent 6890 gas chromatograph (GC) equipped with a flame ionization detector (FID) and thermal conductivity detector (TCD). The weight of the liquid product was obtained through weighing. The Agilent 6890 gas chromatograph was employed to simulate real boiling point distillation and determined the distillation range of liquid products. Gasoline referred to C_5–221 °C fraction, diesel referred to 222–330 °C fraction, and heavy oil referred to fractions > 331 °C. The mass percentage of each fraction could also be obtained. For the gasoline, PIONA analysis was performed, and a hydrocarbon composition in the C_5–C_{12} range was obtained.

Dry gas comprised H_2, CH_4, and C_2 hydrocarbons in the product. LPG was C_3 and C_4 hydrocarbons.

The conversion rate (x) of FT wax was calculated using Equation (1), and the diesel fraction (LCO) and heavy oil fraction (HCO) were considered as reaction materials, in accordance with the practices applied in the FCC process.

$$x = (1 - m1/m - m2/m) \times 100\% \quad (1)$$

$m1$, $m2$, and m were the masses of diesel fraction (LCO), heavy oil fraction (HCO), and raw material FT wax in the reaction material, respectively.

The yield of each fraction was calculated used the following equation:

$$y = m3/m \times 100\% \quad (2)$$

$m3$ is the mass of the product.

The hydrogen transfer index, C_{HT}, was calculated by:

$$C_{HT} = V(iC_4^0)/V(iC_4^=) \quad (3)$$

$V(iC_4^0)$ was the volume fraction of *i*-butane in the gas products and $V(iC_4^=)$ was the *i*-butene's fraction.

5. Conclusions

The influences of the zeolite type, Si/Al ratio of ZSM-5, and the effect of the reaction condition were investigated in detail in the FT wax catalytic cracking reaction.

There were significant differences in the product distribution on the different types of zeolite catalysts. A high selectivity of gasoline and diesel was obtained using the catalyst with USY, which was due to the large cavities of USY. Using the ZSM-5 zeolite catalyst resulted in a high selectivity of dry gas and LPG, owing to its narrow channel, which limited the diffusion of the reaction intermediate and strengthened the cracking reaction. The unique pore structure of the β zeolites promoted the generation of butenes.

The Si/Al ratio of ZSM-5 influenced the conversion of the FT wax and its product distribution. Increasing the ratio promoted the cracking reaction of the FT wax and inhibited the hydrogen transfer reaction, which led to an increase in the light olefins yield. When the Si/Al ratio was 140, the highest reported yields of ethylene, propylene, and butenes were 6.40%, 26.83%, and 20.10%, respectively.

The extension of the reaction time enhanced the conversion of the FT wax, which was conducive to the conversion of gasoline and diesel to dry gas and LPG. Light olefins were generated through both the primary cracking of the FT wax and the secondary cracking of the reaction intermediates.

Author Contributions: C.Y.: investigation, writing the original draft of the manuscript, and analyzed the data. L.L.: collected references, prepared figures, analyzed the data, and writing—review and editing, G.Z. and C.X.: gave valuable advice. X.Z. (Xiance Zhang) and X.Z. (Xiaoqiao Zhang): analyzed the data and editing, writing. All authors have read and agreed to the published version of the manuscript.

Funding: This work was financially supported by a research grant from Sinopec (Fund No. 113017).

Data Availability Statement: Data will be made available on request.

Conflicts of Interest: The authors declare no conflict of interest.

References

1. Li, C.; Wang, G. Dehydrogenation of light alkanes to mono-olefins. *Chem. Soc. Rev.* **2021**, *50*, 4359–4381. [CrossRef]
2. Chen, S.; Chang, X.; Sun, G.; Zhang, T.; Xu, Y.; Wang, Y.; Pei, C.; Gong, J. Propane dehydrogenation: Catalyst development, new chemistry, and emerging technologies. *Chem. Soc. Rev.* **2021**, *50*, 3315–3354. [CrossRef]
3. Hu, Z.; Yang, D.; Wang, Z.; Yuan, Z. State-of-the-art catalysts for direct dehydrogenation of propane to propylene. *Chin. J. Catal.* **2019**, *40*, 1233–1254. [CrossRef]
4. Bricker, J.C. Advanced catalytic dehydrogenation technologies for production of olefins. *Top. Catal.* **2012**, *55*, 1309–1314. [CrossRef]
5. Yang, M.; Fan, D.; Wei, Y.; Tian, P.; Liu, Z. Recent progress in methanol-to-olefins (mto) catalysts. *Adv. Mater.* **2019**, *31*, 1902181. [CrossRef]
6. Gogate, M.R. Methanol-to-olefins process technology: Current status and future prospects. *Petrol. Sci. Technol.* **2019**, *37*, 559–565. [CrossRef]
7. Xu, S.; Zhi, Y.; Han, J.; Zhang, W.; Wu, X.; Sun, T.; Wei, Y.; Liu, Z. Advances in catalysis for methanol-to-olefins conversion. *Adv. Catal.* **2017**, *61*, 37–122.
8. Tian, P.; Wei, Y.; Ye, M.; Liu, Z. Methanol to olefins (mto): From fundamentals to commercialization. *ACS Catal.* **2015**, *5*, 1922–1938. [CrossRef]
9. Chen, J.Q.; Bozzano, A.; Glover, B.; Fuglerud, T.; Kvisle, S. Recent advancements in ethylene and propylene production using the uop/hydro mto process. *Catal. Today* **2005**, *106*, 103–107. [CrossRef]
10. Corma, A.; Corresa, E.; Mathieu, Y.; Sauvanaud, L.; Al-Bogami, S.; Al-Ghrami, M.S.; Bourane, A. Crude oil to chemicals: Light olefins from crude oil. *Catal. Sci. Technol.* **2017**, *7*, 12–46. [CrossRef]
11. Meyers, R.A. *Chemical Engineering Handbook of Petroleum Refining*; McGraw-Hill: New York, NY, USA, 1997.
12. Li, Z.; Jiang, F.; Xie, C.; Xu, Y. DCC technology and its commercial experience. *China Pet. Process. Petrochem. Technol.* **2000**, *9*, 16–22.
13. Li, Z.; Shi, W.; Wang, X.; Jiang, F. Deep catalytic cracking process for light-olefins production. *ACS Symp. Ser.* **1994**, *571*, 33–42.
14. Li, Z.T.; Shi, W.Y.; Pan, R.N.; Jiang, F.K. DCC flexibility for isoolefins production. *Prepr.—Am. Chem. Soc. Div. Pet. Chem.* **1993**, *38*, 581.
15. Scherzer, J. Designing FCC catalysts with high-silica y zeolites. *Appl. Catal.* **1991**, *75*, 1–32. [CrossRef]

16. Rahimi, N.; Karimzadeh, R. Catalytic cracking of hydrocarbons over modified zsm-5 zeolites to produce light olefins: A review. *Appl. Catal. A Gen.* **2011**, *398*, 1–17. [CrossRef]
17. Humphries, A.; Cooper, C.; Seidel, J. *Increasing Butylenes Production from the FCC Unit through Rive's Molecular Highway Technology*; American Fuel & Petrochemical Manufacturers: Washington, DC, USA, 2015.
18. Benton, S. FCC catalyst increases isobutylene yield at European refinery. *Oil Gas J.* **1995**, *93*, 98.
19. Liu, Z.; Shi, S.; Li, Y. Coal liquefaction technologies—Development in China and challenges in chemical reaction engineering. *Chem. Eng. Sci.* **2010**, *65*, 12–17. [CrossRef]
20. Schulz, H. Short history and present trends of fischer–tropsch synthesis. *Appl. Catal. A Gen.* **1999**, *186*, 3–12. [CrossRef]
21. Leckel, D. Diesel production from fischer–tropsch: The past, the present, and new concepts. *Energy Fuel.* **2009**, *23*, 2342–2358. [CrossRef]
22. Khodakov, A.Y.; Chu, W.; Fongarland, P. Advances in the development of novel cobalt fischer–tropsch catalysts for synthesis of long-chain hydrocarbons and clean fuels. *Chem. Rev.* **2007**, *107*, 1692–1744. [CrossRef]
23. Dry, M.E. High quality diesel via the fischer–tropsch process—A review. *J. Chem. Technol. Biotechnol.* **2001**, *77*, 43–50. [CrossRef]
24. Ye, R.; Ding, J.; Gong, W.; Argyle, M.D.; Zhong, Q.; Wang, Y.; Russell, C.K.; Xu, Z.; Russell, A.G.; Li, Q.; et al. CO_2 hydrogenation to high-value products via heterogeneous catalysis. *Nat. Commun.* **2019**, *10*, 5968. [CrossRef] [PubMed]
25. Gao, P.; Zhang, L.; Li, S.; Zhou, Z.; Sun, Y. Novel heterogeneous catalysts for CO_2 hydrogenation to liquid fuels. *ACS Cent. Sci.* **2020**, *6*, 1657–1670. [CrossRef] [PubMed]
26. Gao, P.; Li, S.; Bu, X.; Dang, S.; Liu, Z.; Wang, H.; Zhong, L.; Qiu, M.; Yang, C.; Cai, J.; et al. Direct conversion of CO_2 into liquid fuels with high selectivity over a bifunctional catalyst. *Nat. Chem.* **2017**, *9*, 1019–1024. [CrossRef]
27. Corrao, E.; Salomone, F.; Giglio, E.; Castellino, M.; Ronchetti, S.M.; Armandi, M.; Pirone, R.; Bensaid, S. CO_2 conversion into hydrocarbons via modified fischer–tropsch synthesis by using bulk iron catalysts combined with zeolites. *Chem. Eng. Res. Des.* 2023; *in press*. [CrossRef]
28. Bouchy, C.; Hastoy, G.; Guillon, E.; Martens, J.A. Fischer–tropsch waxes upgrading via hydrocracking and selective hydroisomerization. *Oil Gas Sci. Technol.* **2009**, *64*, 91–112. [CrossRef]
29. de Klerk, A. Fischer–tropsch refining: Technology selection to match molecules. *Green Chem.* **2008**, *10*, 1249–1279. [CrossRef]
30. Leckel, D. Low-pressure hydrocracking of coal-derived fischer–tropsch waxes to diesel. *Energy Fuel.* **2007**, *21*, 1425–1431. [CrossRef]
31. Leckel, D.; Liwanga-Ehumbu, M. Diesel-selective hydrocracking of an iron-based fischer–tropsch wax fraction (c15–c45) using a moo3-modified noble metal catalyst. *Energy Fuel.* **2006**, *20*, 2330–2336. [CrossRef]
32. Dupain, X.; Krul, R.A.; Schaverien, C.J.; Makkee, M.; Moulijn, J.A. Production of clean transportation fuels and lower olefins from fischer–tropsch synthesis waxes under fluid catalytic cracking conditions. *Appl. Catal. B Environ.* **2006**, *63*, 277–295. [CrossRef]
33. Dupain, X.; Krul, R.A.; Makkee, M.; Moulijn, J.A. Are fischer–tropsch waxes good feedstocks for fluid catalytic cracking units? *Catal. Today* **2005**, *106*, 288–292. [CrossRef]
34. Komvokis, V.G.; Karakoulia, S.; Iliopoulou, E.F.; Papapetrou, M.C.; Vasalos, I.A.; Lappas, A.A.; Triantafyllidis, K.S. Upgrading of fischer–tropsch synthesis bio-waxes via catalytic cracking: Effect of acidity, porosity and metal modification of zeolitic and mesoporous aluminosilicate catalysts. *Catal. Today* **2012**, *196*, 42–55. [CrossRef]
35. Yang, M.; Wang, G.; Han, J.; Gao, C.; Gao, J. Fischer–tropsch wax catalytic cracking for the production of low olefin and high octane number gasoline: Process optimization and heat effect calculation. *Petrol. Sci.* **2023**, *20*, 1255–1265. [CrossRef]
36. Zhao, W.; Wang, J.; Song, K.; Xu, Z.; Zhou, L.; Xiang, H.; Hao, X.; Yang, Y.; Li, Y. Eight-lumped kinetic model for fischer–tropsch wax catalytic cracking and riser reactor simulation. *Fuel* **2022**, *308*, 122028. [CrossRef]
37. Guangtao, S.; Meng, J.; Hao, H.; Hua, Y. Research on calculation of molecular diameter and molecular distillation separation of f-t wax. *Pet. Refin. Eng.* **2022**, *52*, 57–61.
38. Konno, H.; Okamura, T.; Kawahara, T.; Nakasaka, Y.; Tago, T.; Masuda, T. Kinetics of n-hexane cracking over zsm-5 zeolites—Effect of crystal size on effectiveness factor and catalyst lifetime. *Chem. Eng. J.* **2012**, *207–208*, 490–496. [CrossRef]
39. Mochizuki, H.; Yokoi, T.; Imai, H.; Watanabe, R.; Namba, S.; Kondo, J.N.; Tatsumi, T. Facile control of crystallite size of zsm-5 catalyst for cracking of hexane. *Micropor. Mesopor. Mat.* **2011**, *145*, 165–171. [CrossRef]
40. Hirota, Y.; Murata, K.; Miyamoto, M.; Egashira, Y.; Nishiyama, N. Light olefins synthesis from methanol and dimethylether over sapo-34 nanocrystals. *Catal. Lett.* **2010**, *140*, 22–26. [CrossRef]
41. Bjorgen, M.; Svelle, S.; Joensen, F.; Nerlov, J.; Kolboe, S.; Bonino, F.; Palumbo, L.; Bordiga, S.; Olsbye, U. Conversion of methanol to hydrocarbons over zeolite h-zsm-5: On the origin of the olefinic species. *J. Catal.* **2007**, *249*, 195–207. [CrossRef]
42. Mota, C.J.A.; Rawet, R. Mechanism of aromatic hydrocarbon formation in FCC naphtha. *Ind. Eng. Chem. Res.* **1995**, *34*, 4326–4332. [CrossRef]
43. Rice, F.O. The thermal decomposition of organic compounds from the standpoint of free radicals. III. The calculation of the products formed from paraffin hydrocarbons. *J. Am. Chem. Soc.* **1933**, *55*, 3035–3040. [CrossRef]
44. Rice, F.O. The thermal decomposition of organic compounds from the standpoint of free radicals. I. Saturated hydrocarbons. *J. Am. Chem. Soc.* **1931**, *53*, 1959–1972. [CrossRef]

45. Wang, L.; Peng, B.; Zheng, A.; Song, Y.; Jiang, Q.; Wang, P.; Song, H.; Lin, W.; He, M. Mechanistic origin of transition metal modification on zsm-5 zeolite for the ethylene yield enhancement from the primary products of n-octane cracking. *J. Catal.* **2022**, *416*, 387–397. [CrossRef]
46. Emeis, C.A. Determination of integrated molar extinction coefficients for infrared absorption bands of pyridine adsorbed on solid acid catalysts. *J. Catal.* **1993**, *141*, 347–354. [CrossRef]